OPTIMAL DETECTION OF MULTIHARMONIC VISUALLY EVOKED POTENTIALS

Carlos E. Davila [1]   Richard Srebro [2]   Ibrahim A. Ghaleb [1] *

[1] Electrical Engineering Department, Southern Methodist University, Dallas, Texas, USA
[2] Department of Ophthalmology, University of Texas Southwestern Medical Center, Dallas, Texas, USA

ABSTRACT

We consider the problem of detecting visual evoked potentials (VEP's). A matched subspace filter is applied to the detection of the VEP and is demonstrated to perform better than a number of other evoked potential (EP) detectors. Unlike single-harmonic detectors, the MSF detector is suitable for detecting multi-harmonic VEP's. Moreover, the MSF is optimal in the uniformly most powerful (UMP) sense for multi harmonic signals with unknown noise variance.

1. BACKGROUND

Visual grating acuity (GA) is useful in the clinical evaluation of patients with eye and neurologic disease. Grating acuity is obtained by having the subject view a contrast grating at a fixed contrast (usually 100%) while the spatial frequency is increased until the subject can no longer detect the contrast grating. In adults, measurements can be accomplished psychophysically; however infants, young children, and non-verbal patients can not be studied with psychophysical methods. Several researchers have proposed using the steady state visual evoked potential (VEP) as an objective method of determining GA [1, 2, 3]. Most of these methods utilize the second harmonic of stimulus contrast reversal frequency to detect the presence of a VEP. The generalized T^2 statistic [4], the T^2_{circ} statistic [5, 6] and the Rayleigh Phase Criterion (RPC) by [7], are representative of these types of detection algorithms. All of the above statistics are parametric in the sense that they assume that under the null hypothesis, the noise (EEG) has a Gaussian density. This assumption has been found to be reasonable by several investigators [8, 9]. The ROTP detector looks at the power in ensemble averages derived via all possible sign permutations of the data frames. If the average corresponding to all + signs (i.e. no sign changes) is in the top 5-percentile of all possible ensemble average powers, a detection is made, hence this detector is non-parametric [10].

Victor and Mast compared the RPC, T^2, and T^2_{circ} statistics and found that their T^2_{circ} statistic outperformed the others [5]. One drawback of all of these statistics is that they are all based on the second harmonic of the contrast reversal frequency; there is no reason to expect near-threshold EP's to contain only the second harmonic, and if other signal harmonics are present, then current methodology does not appear to have exploited them.

2. MATCHED SUBSPACE FILTERING

Throughout this paper, we shall consider detection based on an M-dimensional measurement vector x consisting of a signal and an additive noise component. In EP detection, the vector x arises from taking M samples of an EEG signal during a psychophysical GA experiment (see Section 5.). Assume that the measurement model is given by $x = s + z$ where x, s, and z are M-vectors corresponding to the measurement, the signal component, and an additive noise component, respectively. Often, one does not know the exact morphology of the signal. If the signal vector is known only to lie within a given subspace, then it can be expressed as

$$s = \sum_{k=1}^{2N} \alpha_k s_k \qquad (1)$$

where the s_k are known vectors and the α_k are unknown. The signal vector can therefore be said to lie in a signal subspace, defined as the column space of

$$S = [\ s_1 \quad s_2 \quad \cdots \quad s_{2N}\ ] \qquad (2)$$

The Matched Subspace Filter (MSF) detector has an $F(2N, M - 2N)$ distribution [11]

$$\frac{M - 2N}{2N} \frac{x^T P_S x}{x^T (I - P_S) x} \qquad (3)$$

where

$$P_S = S(S^T S)^{-1} S^T \qquad (4)$$

is the projection matrix into the range of S. The MSF detector is optimal in the uniformly most powerful (UMP) sense if the signal model $y = s + z$ satisfies:

- Variance of Gaussian white noise z is unknown.
- Signal vector s lies in a known subspace

The MSF detector appears to be ideally suited for detection of low-level VEP's if a multi-harmonic signal model is assumed. The signal subspace can then be considered to be the span of vectors associated with a finite number of even harmonics of the temporal stimulus frequency. In order to get white noise, the EEG background must be prewhitened.

3. VEP SIGNAL MODEL

We assume that the signal component consists of N even harmonics of the contrast reversal frequency. Let $s_k(n)$ be the nth entry of the signal subspace vector s_k

$$s_k(n) = cos(2\pi f_k n), \quad k = 1, 2, \ldots, N \qquad (5)$$

$$s_k(n) = sin(2\pi f_{k-N} n), \quad k = N+1, N+2, \ldots, 2N \quad (6)$$

and $f_k = 2k \times f_{stim}, k = 1, 2, \ldots, N$ where f_{stim} is the contrast reversal frequency. It is well known that the counter phase modulated contrast grating stimulus paradigm produces only even harmonics of the contrast reversal frequency. The measurement noise vector z represents additive EEG "noise" and is assumed to consist of a discrete-time AR random process,

$$z[n] = -\sum_{k=1}^{p} a_k z[n-k] + u[n] \quad (7)$$

where $u[n]$ is white Gaussian noise. This model for the noise allows one to easily design a whitening filter based on a forward linear predictor. It can be shown that the presence of low-level sinusoids has a very limited effect on the whitening filter derived via the Yule-Walker equations for linear prediction [12].

4. WHITENING FILTER DESIGN

An autoregressive random process of order p ($AR(p)$) can by whitened by filtering it with the FIR filter

$$w^* = [\begin{array}{ccccc} 1 & a_1 & a_2 & \ldots & a_p \end{array}] \quad (8)$$

In practice, the whitening filter is found by estimating the parameters of the $AR(p)$ process using the Yule-Walker equations for forward linear prediction [12]. The whitening filter then becomes

$$w = [\begin{array}{ccccc} 1 & \hat{a}_1 & \hat{a}_2 & \ldots & \hat{a}_p \end{array}] \quad (9)$$

where $\hat{a}_k, k = 1, \ldots, p$ are the AR parameter estimates. Note that in general, $w \neq w^*$ since w is based on sample autocorrelation functions. However, w is unbiased for the autocorrelation method of solving the Yule-Walker equations [12]. If the $AR(p)$ process also contains low-level sinusoids, these will produce biased parameter estimates and the resulting whitening filter w will be suboptimal (i.e. it will not whiten). Nevertheless, if the bias is sufficiently small, then the whitening properties of w are relatively unaffected. We shall prove that the presence of low-level sinusoids produces a small bias in the whitening filter.

The Yule-Walker equations for the AR parameters are given by

$$R_{zz}\tilde{w} = b \quad (10)$$

where

$$R_{zz} = \begin{bmatrix} r_{zz}[0] & r_{zz}[-1] & \cdots & r_{zz}[p] \\ r_{zz}[1] & r_{zz}[0] & \cdots & r_{zz}[p-1] \\ \vdots & \vdots & \ddots & \vdots \\ r_{zz}[p] & r_{zz}[p-1] & \cdots & r_{zz}[0] \end{bmatrix} \quad (11)$$

$$b = [\begin{array}{cccc} 1 & 0 & \cdots & 0 \end{array}]^T \quad (12)$$

$$\tilde{w} = \beta [\begin{array}{ccccc} 1 & a_1 & a_2 & \cdots & a_p \end{array}]^T \quad (13)$$

and $r_{zz}[k]$ is the autocorrelation function of the AR process. The scalar constant β accounts for the fact that the first element of b is unity rather than the variance of $u[n]$. We shall consider the bias due to the presence of a single sinusoid. We also assume that the autocorrelation estimates used in the Yule-Walker equations are "close" to the true autocorrelation function, $\hat{r}_{zz}[k] \approx r_{zz}[k]$ which allows us to check only the biasing effect of the sinusoid. Due to the presence of the sinusoid, R_{zz} is perturbed by the autocorrelation matrix associated with the sinusoid,

$$R_{ss} =$$
$$\frac{A^2}{2} \begin{bmatrix} 1 & cos(2\pi f_o) & \ldots & cos(2\pi f_o p) \\ cos(2\pi f_o) & 1 & \ldots & cos(2\pi f_o(p-1)) \\ \vdots & \vdots & \ddots & \vdots \\ cos(2\pi f_o p) & cos(2\pi f_o(p-1)) & \ldots & 1 \end{bmatrix}$$
$$(14)$$

The Yule-Walker Equations become

$$(R_{zz} + R_{ss})(\tilde{w} + \delta\tilde{w}) = b \quad (15)$$

the quantity $\delta\tilde{w} = \beta\delta w$ represents the bias in the Yule-Walker equation solution due to the presence of R_{ss}. The quantity δw is the bias that results in the Yule-Walker equations when the first element of b is replaced by the variance of $u[n]$. Perturbation theory for a system of linear equations can be used to establish a bound for the bias δw. Assuming,

$$\|R_{zz}^{-1}\|\|R_{ss}\| < 1 \quad (16)$$

where $\|\cdot\|$ is any matrix norm, then it can be shown that

$$\frac{\|\delta\tilde{w}\|}{\|\tilde{w}\|} \leq \frac{\|R_{zz}^{-1}\|\|R_{ss}\|}{1 - \|R_{zz}^{-1}\|\|R_{ss}\|} \quad (17)$$

If $\|R_{zz}^{-1}\|\|R_{ss}\| \ll 1$, which is satisfied for low SNR, and since $\|\delta\tilde{w}\|/\|\tilde{w}\| = \|\delta w\|/\|w\|$, (17) becomes,

$$\frac{\|\delta w\|}{\|w\|} \leq \|R_{zz}^{-1}\|\|R_{ss}\| \quad (18)$$

The quantity $\|R_{zz}^{-1}\|\|R_{ss}\|$ is related to, but generally not equal to the SNR. When the sinusoid power is very low relative to the power in the $AR(p)$ process then the relative bias $\|\delta w\|/\|w\|$ becomes very small.

The power spectral density estimate of a high SNR VEP signal is shown in Fig. 1 before and after the AR pre-whitener. The PSD's were obtained by averaging 25 periodograms derived from 864-point trials. A different whitening filter was computed for each 864-point trial. The figure illustrates the effectiveness of the AR filter in producing a flatter spectrum while preserving the evoked stimulus harmonics.

5. METHODS

The stimuli were black and white vertical square wave gratings with contrast at 92%. These were created on a video monitor using a high resolution graphics board (Omnicomp, Texan ET, 1280 by 1024 pixels, 60 Hz, non-interleaved). The subjects viewed the video monitor binocularly from a distance of 3 m in a darkened room. The video screen was masked to reveal a 5.5 degree circular field. A small fixation dot was placed at the center of th display. The luminance of the display was approximately 30 Foot Lamberts. Counter-phase contrast reversal (3.75 Hz, 7.5 reversals per sec, square wave modulation) was used as the basic stimulus. Spatial frequencies from 4 to 40 c/d (4, 8, 10, 13, 16, 20, 24, 28 and 40 c/d) were viewed in different runs. The selection of a spatial frequency for a particular run was randomized for each subject. Each run consisted of the continuous counter-phase stimulus for 173 s. An experimental session consisted of 19 such runs with each spatial frequency

being shown twice except for the 40 c/d stimulus which was shown three times. The 40 c/d stimulus was seen by the subject as an homogeneous field. None of the subjects could either detect the grating or detect any difference between this stimulus and a true homogeneous field. In addition, we ran several control experiments to compare the VEP's due to a 40 c/d reversing grating with 92% contrast and 0% contrast. There was no detectable difference, neither stimulus produced a measurable VEP.

Electrodes were placed on the scalp at O_z (10-20 international system, over visual cortex) and at the vertex. The active electrode was at O_z and the vertex electrode served as the reference. A ground electrode was placed on the ear or mastoid. The EEG was amplified (10^5), analog filtered (0.1 to 100 Hz, single stage Butterworth), digitized at 200 Hz and streamed to disk. The EEG acquisition was done under Lab-View control. A separate channel was used to acquire a square wave monitor signal which was time-locked to the grating reversal.

Fourteen normal volunteers served as subjects with informed consent obtained according to an IRB approved protocol (Southwestern Medical School). All subjects were adults with normal visual acuity.

6. DATA ANALYSIS

Each fixed spatial-frequency run consisted of 25 sets of $M = 864$-sample measurement vectors. Each of the 25 measurement vectors was prewhitened with a $p = 15$-order whitening filter. Next, each of the 25 prewhitened measurement vectors was submitted for detection analysis via each of the following detection methods:

- RPC
- generalized T^2
- generalized T_{circ}^2
- ROTP
- MSF

For each measurement vector, a decision was made, and the probability of detection was estimated as the percentage of detections per run. The threshold for making a decision was based on a 5% probability of false alarm and the assumed probability density functions for the null hypothesis for each detector. The ROTP detector should generate a false alarm probability of 5% and makes no assumptions about the noise probability density. The estimated probability of detection P_D was then averaged across the 14 subjects and plotted as a function of spatial frequency for each detector. The results are shown in Fig. 2. The MSF detector is seen to have considerably higher probability of detection relative to the other detectors. Table I shows the mean and standard deviations for each detector averaged across all no-signal (40 c/d) runs. All means are close to, though below the theoretical false alarm probability of 5%.

7. DISCUSSION

A matched subspace filter (MSF) was applied to the detection of VEP's and was found to outperform a number of other evoked potential detectors including one (T_{circ}^2) commonly used in human application [5]. The MSF detector has been shown to be optimal (uniformly most powerful, UMP) for the detection of multi-harmonic signals in zero-mean Gaussian white noise having unknown variance [11].

Detector	Mean P_D	P_D Standard Deviation
ROTP	3.55	2.70
RPC	2.69	2.70
T^2	3.85	3.32
T_{circ}^2	3.49	2.78
MSF	4.67	2.35

Table 1. Mean and standard deviations of probability of detection P_D at the 40 c/d noise-only case for each detector. Thresholds were set to give 5% false alarm probability.

REFERENCES

[1] D. Regan, "Speedy assessment of visual acuity in amblyopia," *Ophthalmogica*, vol. 175, pp. 159–164, 1977.

[2] C. Tyler, P. Apkarian, D. Levi, and K. Nakayama, "Rapid assessment of visual function: an electronic sweep technique for pattern evoked potential," *Invest. Ophthalmol. Vis. Sci.*, vol. 18, pp. 703–713, 1979.

[3] D. Weiner, K. Wellish, J. Nelson, and M. Kupersmith, "Comparisons among snellen, psychophysical and evoked potential acuity determinations," *Am. J. Optom. Physiol. Opt.*, vol. 62, pp. 669–679, 1985.

[4] T. W. Anderson, *An Introduction to Multivariate Statistical Analysis*. Wiley, 1984.

[5] J. Victor and J. Mast, "A new statistic for steady-state evoked potentials," *Electroencephalography and Clinical Neurophysiology*, vol. 78, pp. 378–388, 1991.

[6] J. Mast and J. Victor, "Fluctuations of steady-state veps: Interaction of driven evoked potentials and the eeg," *Electroencephalography and Clinical Neurophysiology*, vol. 78, pp. 389–401, 1991.

[7] K. V. Mardia, *Statistics of Directional Data*. Academic Press, Inc., New York, 1972.

[8] J. McEwen and G. Anderson, "Modeling the stationarity and gaussianity of spontaneous electroencephalographic activity," *IEEE Trans. Biomed. Eng.*, vol. BME-22, pp. 361–369, Sept. 1975.

[9] T. Gasser, J. Möcks, and W. Köhler, "Amplitude probability distribution of noise for flash-evoked potentials and robust response estimates," *IEEE Trans. Biomed. Eng.*, vol. BME-33, pp. 579–584, June 1986.

[10] A. Achim, "Signal detection in averaged evoked potentials: Monte carlo comparison of the sensitivity of different methods," *Electroencephalography and Clinical Neurophysiology*, vol. 96, pp. 574–584, 1995.

[11] L. Scharf, *Statistical Signal Processing*. Addison-Wesley, 1991.

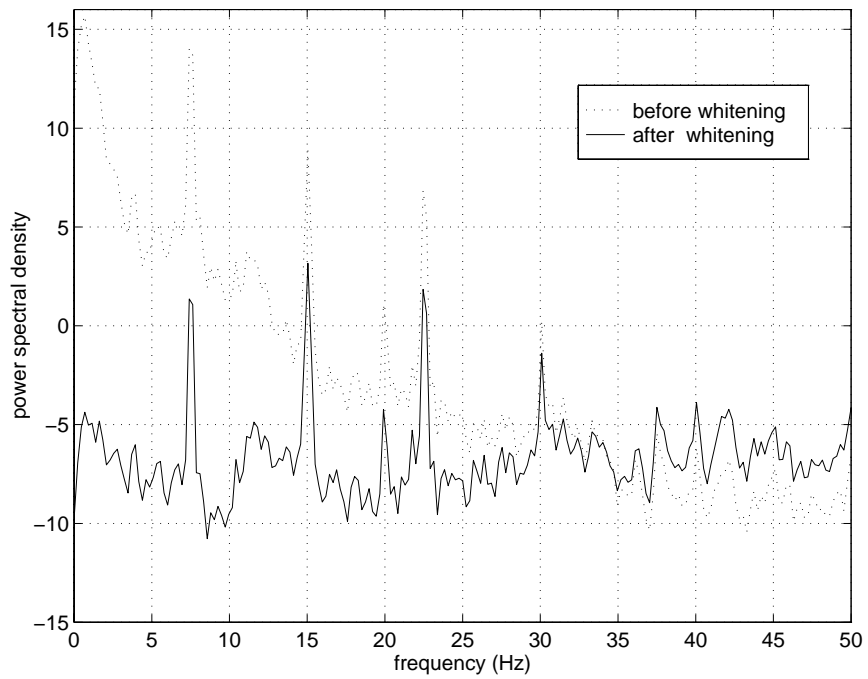[12] S. Kay, *Modern Spectral Estimation*. Prentice Hall, 1988.

Figure 1. The power spectral density of the VEP with and without pre-whitening.

Figure 2. Probability of detection averaged across subjects.